Surface defect gap solitons in two-dimensional optical lattices*

Meng Yun-Ji(孟云吉), Liu You-Wen(刘友文)†, and Tang Yu-Huang(唐宇煌)

Department of Applied Physics, Nanjing University of Aeronautics and Astronautics, Nanjing 210016, *China*

(Received 28 November 2011; revised manuscript received 7 December 2011)

We investigate the existence and stability of surface defect gap solitons at an interface between a defect in a two-dimensional optical lattice and a uniform saturable Kerr nonlinear medium. The surface defect embedded in the two-dimensional optical lattice gives rise to some unique properties. It is interestingly found that for the negative defect, stable surface defect gap solitons can exist both in the semi-infinite gap and in the first gap. The deeper the negative defect, the narrower the stable region in the semi-infinite gap will be. For a positive defect, the surface defect gap solitons exist only in the semi-infinite gap and the stable region localizes in a low power region.

Keywords: surface defect gap soliton, optical lattice, saturable Kerr nonlinear media

PACS: 42.65.Tg, 42.65.Jx, 42.65.Wi **DOI:** 10.1088/1674-1056/21/7/074206

1. Introduction

Surface waves, localized waves propagating at the interface separated by two media with different properties, are ubiquitous wave phenomena in optics. Owing to their unique features of having no analogues in bulk, surface waves have been found to possess potential applications in the exploration of the surface characteristics of optical materials. In the linear optical domain, the surface modes at the interface between uniform and periodically layered media began to be studied long time ago.[1] Recently, the research interest in this domain was renewed after the metamaterial had been used to construct multilayered media.[2]

In the nonlinear optical domain, the studies of the surface waves pinned to interfaces between different nonlinear optical media, at least one of which carries a lattice structure, have also attracted intense attention.[3−10] Extensive theoretical and experimental investigations have been carried out in the context of obtaining stable surface solitons in diverse settings. In one-dimensional (1D) arrays, the Kerr surface solitons near the edge of a semi-infinite waveguide with self-focusing nonlinearity were theoretically predicted and experimentally observed by Makris *et al.*[3] and Suntsov *et al.*[4] for the first time. They also found that surface solitons can exist at the heterointerface between two dissimilar semi-infinite 1D waveguide arrays, as well as at the boundaries of a two-dimensional (2D) nonlinear lattice.[5] In addition, Kartashov *et al.*[6] suggested the existence of surface gap solitons at the interface separated by uniform media and an optical lattice (OL) with self-defocusing nonlinearity, which was observed in semi-infinite waveguide arrays.[7] In 2D arrays, the theoretical prediction of the edge and corner solitons inspired two experiments, one in asymmetric waveguide arrays of Kerr type (fused silica)[8] and the other in a photorefractive medium.[9] Apart from the above two experiments, one should note that Szameit *et al.*[10] reported on the observation of 2D surface solitons at the interface between square and hexagonal waveguides. In addition, the nonlocal surface-wave solitons occurring at the interface between a dielectric medium (air) and a nonlinear material with a long-range nonlocal response were demonstrated theoretically and experimentally by Alfassi *et al.*[11] Surface solitons at the interface between a 1D photonic superlattice and a uniform medium with weak nonlocal nonlinearity were also proposed.[12]

Defect modes (DMs) in photonic lattices have also been considered in Refs. [13]–[22]. Fedele *et al.*[13] investigated the linear DMs in 1D photonic lattices and found that a variety of DMs in the negative (repulsive) defect case. The nonlinear 1D defect DMs (defect solitons) and their stability were studied by Yang

*Project supported by the National Natural Science Foundation of China (Grant No. 11174147) and the Natural Science Foundation of Jiangsu Province, China (Grant No. BK2009366).

†Corresponding author. E-mail: ywliu@nuaa.edu.cn

© 2012 Chinese Physical Society and IOP Publishing Ltd

and Chen[14] in detail. One of the striking results in their work is that for a repulsive defect, defect solitons in the first gap are linearly stable, while the reverse scenario is found in the attractive case. In the 2D geometry, linear and nonlinear localized DMs were systematically studied by Wang *et al.*[15] and Chen *et al.*[16] respectively. The defect solitons in Kagome OLs were also reported.[17] Apart from the above work concentrating on the single-site defect, defect solitons, and their stability in a defect that covers several lattice sites have also been studied.[18,19] Motivated by the above theoretical predictions, some typical experiments have been performed to observe defect modes in 1D negative defects[20] and 2D negative defects in optically-induced OLs,[21] as well as 2D negative and positive defects in a hexagonal waveguide array.[22]

Surface defect gap solitons (SDGSs) have been analysed in 1D simple lattices[23] and dual-frequency lattices.[24] Despite the above progress, SDGSs in 2D geometry are still poorly understood. In the present work, we report the existence and stability of the surface defect gap solitons at an interface between a defect of 2D OLs and uniform saturable Kerr nonlinear media. For the repulsive defect, SDGSs with moderate power could stably exist in the semi-infinite (SI) gap (corresponding to the first gap in Ref. [23]). What is worth emphasizing is that for some specific repulsive defect, SDGSs can stably exist in the whole first gap (corresponding to the second gap in Ref. [23]). For the attractive defect, SDGSs exist only in SI gaps and are stable in the low power region.

2. Theoretical modeling

To elucidate the dynamics of the beam propagating at the interface between uniform and two-dimensional OLs with a single defect embedded in the self-focusing saturable nonlinear medium, we consider the normalized 2D nonlinear Schrödinger equation for the light field q[25]

$$\mathrm{i}\frac{\partial q}{\partial z}+\frac{\partial^2 q}{\partial x^2}+\frac{\partial^2 q}{\partial y^2}-\frac{E_0}{1+I_{\mathrm{L}}+|q|^2}q=0, \qquad (1)$$

where I_{L} is the intensity profile of the OLs with a defect located in the centre of the OLs, $I_{\mathrm{L}}=0$ at $x<-\pi/2$;

$$I_{\mathrm{L}}=I_0\cos^2(x)\cos^2(y)\{1+\varepsilon\exp[-(x^2+y^2)^4/128]\}, \qquad (2)$$

at $x\geq-\pi/2$, with I_0 being the total strength of the OLs; ε the modulation depth of the defect intensity; x and y are transverse coordinates measured in units of D/π, with D being the lattice spacing; z is the propagation distance in units of $2k_1D^2/\pi^2$, where $k_1=k_0n_{\mathrm{e}}$, with $k_0=2\pi/\lambda_0$ being the wave number, λ_0 the wavelength in vacuum, n_{e} the unperturbed refractive index along the extraordinary axis; E_0 is the applied bias field in units of $\pi^2/(k_0^2n_{\mathrm{e}}^4D^2\gamma_{33})$, with γ_{33} being the electro-optic coefficient of the crystal. We set the parameters to be $D=20$ μm, $\lambda_0=0.5$ μm, $n_{\mathrm{e}}=2.3$, and $\gamma_{33}=280$ pm/V.[13] As a consequence, one x or y unit corresponds to 6.4 μm, one z unit corresponds to 2.3 μm, and one E_0 unit corresponds to 20 V/mm. The intensity distribution of the defect lattices are illustrated in Figs. 1(b)–1(d) for zero, negative ($\varepsilon=-0.5$), and positive ($\varepsilon=0.5$) defects, respectively, from which we note that if $\varepsilon<0$ (repulsive), the light intensity I_{L} at the defect site is lower than those at the surrounding sites. In contrast, when $\varepsilon>0$ (attractive), the light intensity I_{L} at the defect site is higher than those at the surrounding sites.

Other parameters are $I_0=3$ and $E_0=6$ (corresponding to a maximal refractive change 2.04×10^{-4} without defect, and a minimal refractive change 0.51×10^{-4} without defect, 0.32×10^{-4} with defect $\varepsilon=0.5$, 0.82×10^{-4} with defect $\varepsilon=-0.5$) which are fixed unless otherwise stated. By illuminating the sample with a broad laser beam passing through a properly designed amplitude mask, the potential given by Eq. (2) can be realized optically in a photorefractive crystal.[25]

First, we utilize the plane-wave expansion method based on the Bloch theorem to obtain the bandgap structure of the system. We substitute $q(x,y,z)=u(x,y)\exp[\mathrm{i}(k_xx+k_yy)-\mathrm{i}\mu z]$ into the linearized expression of Eq. (1), where $u(x,y)$ is the periodic function with the same period as the OLs, k_x and k_y are the Bloch wave-numbers, and μ is the propagation constant. The obtained bandgap spectrum is shown Fig. 1(a), from which we can find that the boundaries and range of the semi-infinite gap and the first gap are $\mu<3.584$ and $4.41<\mu<5.552$, respectively.

Next, we search for the stationary soliton solutions in the form of $q(x,y,z)=u(x,y)\exp(-\mathrm{i}\mu z)$, where $u(x,y)$ is the real function obeying the following nonlinear equation:

$$\frac{\partial^2 u}{\partial x^2}+\frac{\partial^2 u}{\partial y^2}-\frac{E_0}{1+I_{\mathrm{L}}+|u|^2}u=-\mu u. \qquad (3)$$

The power of the soliton is defined as $P=\int_{-\infty}^{\infty}\int_{-\infty}^{\infty}|u|^2\,\mathrm{d}x\,\mathrm{d}y$. Solving Eq. (3) by dint of the modified square-operator iteration method (MSOM) proposed by Yang and Lakoba,[26] we can acquire the soliton profiles.

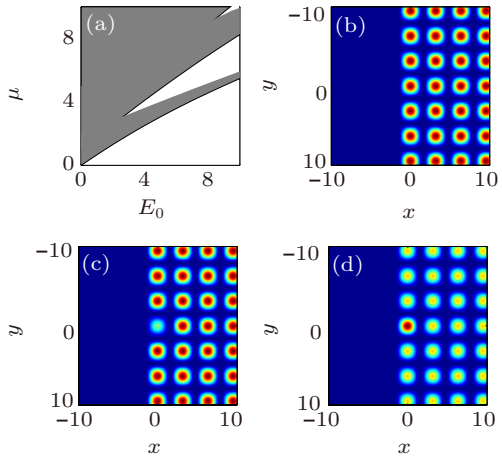


Fig. 1. (colour online) (a) Bandgap spectrum of the square optical lattices. (b) The intensity distribution without a defect. (c) The intensity distribution with a repulsive defect $\varepsilon = -0.5$. (d) The intensity distribution with an attractive defect $\varepsilon = 0.5$.

Lastly, we examine the linear stability of SDGSs by considering the perturbed stationary solution form as

$$\begin{aligned} q(x,y,z) = &\{u(x,y) + [v(x,y) - w(x,y)]\exp(\delta z) \\ &+ [v(x,y) + w(x,y)]^* \exp(\delta^* z)\} \\ &\times \exp(-\mathrm{i}\mu z), \end{aligned}$$

where δ is the associated growth rate, the superscript "$*$" represents complex conjugation, and the perturbed components $v, w \ll 1$. Linearization of Eq. (1) around u yields the eigenvalue problem

$$-\mathrm{i}\begin{pmatrix} 0 & L_0 \\ L_1 & 0 \end{pmatrix}\begin{pmatrix} v \\ w \end{pmatrix} = \delta \begin{pmatrix} v \\ w \end{pmatrix}, \tag{4}$$

$$L_0 = \frac{\partial^2}{\partial x^2} + \frac{\partial^2}{\partial y^2} + \mu - \frac{E_0}{1 + I_\mathrm{L} + |u|^2}, \tag{5}$$

$$\begin{aligned} L_1 = &\frac{\partial^2}{\partial x^2} + \frac{\partial^2}{\partial y^2} + \mu - \frac{E_0}{1 + I_\mathrm{L} + |u|^2} \\ &+ \frac{2E_0 u^2}{(1 + I_\mathrm{L} + |u|^2)^2}. \end{aligned} \tag{6}$$

We solve the above equations by adopting the original operator method (OOM)[27] to find perturbation profiles and associated growth rates. The stability criterion of the system is that if $\mathrm{Re}(\delta) > 0$, the SDGSs are linearly unstable, otherwise they are linearly stable.[27]

3. Numerical simulations and discussion

We first study the repulsive defect case and take $\varepsilon = -0.5$ as a typical example. In such a case, we find that the SDGSs can exist stably in both SI gap and the first gap. The dependence of the total power P on the propagation constant μ is displayed in Fig. 2(a), from which one can draw a conclusion that the soliton power is a monotonically decreasing function of propagation constant with exception of the propagation constant approaching the gap edge. This means that the slope of the P–μ curve is negative when $\mu < 3.55$. According to the Vakhitov–Kolokolov (VK) criterion, i.e., $\mathrm{d}P/\mathrm{d}\mu < 0$ is known as the necessary condition for the stability of solitons supported by the self-focusing nonlinearity,[28] the SDGSs may be stable in a region of $\mu < 3.55$. Moreover, we calculate the dependence of the real part of the growth rate δ on propagation constant μ as shown in Fig. 2(b), and ascertain that the stable SDGSs emerge only in a narrow region i.e., $2.707 < \mu < 3.193$, which accords with the VK criterion. The existence region $2.707 < \mu < 3.193$ of the surface defect gap solitons in this case is narrower than the region $2.42 < \mu < 3.43$ of the defect solitons in the corresponding bulk case.[16] To confirm the predictions of the linear analysis, we solve Eq. (1) with the input condition $q(x, y, z = 0) = u(x, y)[1 + \rho(x, y)]$ by employing the split-step Fourier method, where $\rho(x, y)$ is the random function with Gaussian distribution with its relative amplitude set at 10% level. First, we demonstrate the stable region $2.707 < \mu < 3.193$. For instance, the profile of SDGSs for $\mu = 2.85$ is shown in Fig. 2(c), and the SDGSs are trapped at the defect site and maintain their profiles at $z = 150$ and $z = 300$, as obviously shown in Figs. 2(d) and 2(e), respectively. Next, we turn to one of the unstable regions ($\mu \leq 2.707$), and choose $\mu = 1.75$ as a representative example. The profiles of the SDGSs corresponding to excitations at 0, 150, and 300 unit distances in the nonlinear medium are illustrated in Figs. 2(f)–2(h), respectively. The results reveal that the SDGSs cannot be trapped at the defect site and the VK instability leads to the snakelike position oscillations of the SDGSs. It is worth emphasizing that in this unstable region, the power is even higher and grows exponentially with the decreasing of propagation constant, as shown in Fig. 2(a). Apparently, such instability of the SDGSs in the high power region is different from the usual VK instability caused by a sign change in the slope of the power diagram.[14] Then we study the other unstable region of $3.193 < \mu < 3.58$, in which the P–μ curve is not smooth, as shown in Fig. 2(b). During propagating in the medium, the SDGSs ($\mu = 3.45$) decay as shown in Figs. 3(a)–3(c), which demonstrates great consistence with the analytic prediction shown in the Fig. 2(b). In the first gap, the SDGSs are always stable under perturbations

in their existing region of $4.41 < \mu < 4.83$, and the slope of the P–μ curve is negative, which is in accordance with the VK criterion. The results mentioned above are confirmed by Figs. 3(d)–3(f) ($\mu = 4.45$) and Figs. 3(g)–3(i) ($\mu = 4.75$).

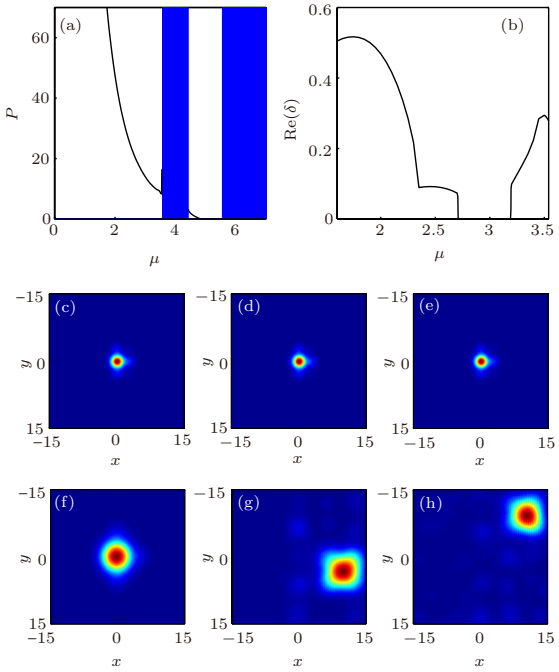


Fig. 2. (colour online) (a) Power diagram of SDGSs (dark regions correspond to Bloch bands). (b) Re(δ) versus μ. (c)–(e) Profiles of SDGS for $\mu = 2.85$ at $z = 0$, 150 and 300 unit distances respectively. (f)–(h) Profiles of SDGS for $\mu = 1.75$ at $z = 0$, 150 and 300 unit distances, respectively. $\varepsilon = -0.5$.

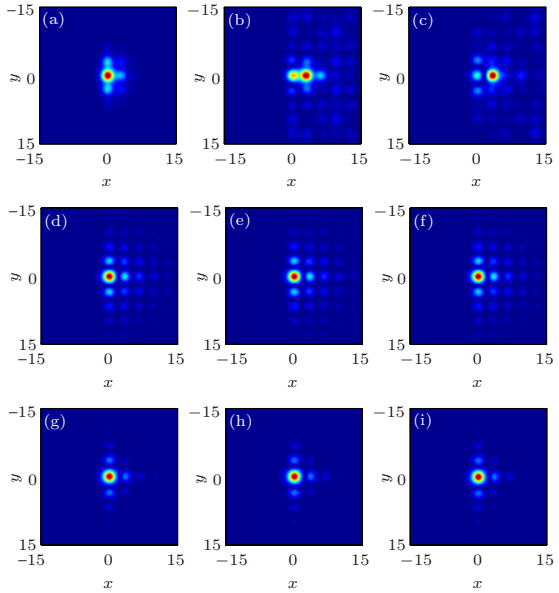


Fig. 3. (colour online) Profiles of SDGS for (a) $\mu = 3.45$, $z = 0$; (b) $\mu = 3.45$, $z = 150$; (c) $\mu = 3.45$, $z = 300$; (d) $\mu = 4.45$, $z = 0$; (e) $\mu = 4.45$, $z = 150$; (f) $\mu = 4.45$, $z = 300$; (g) $\mu = 4.75$, $z = 0$; (h) $\mu = 4.75$, $z = 150$; (i) $\mu = 4.75$, $z = 300$. $\varepsilon = -0.5$.

As a controllable parameter, the influence of the applied electric field E_0 on the stability properties of the SDGSs is investigated. We increase the E_0 value from 6 to 6.5 (while keeping $I_0 = 3$), and obtain the dependence of the real part of the growth rate on propagation constant, which is plotted in Fig. 4. At the higher E_0 value of 6.5, one should note that the upper boundary value of SI gap is $\mu = 3.836$, and accordingly, the stability region of SDGSs becomes broader (i.e., $2.62 < \mu < 3.548$), namely, increasing the applied bias electric field could significantly stabilize the SDGSs. This may be explained physically as follows: with I_0 fixed, the depth of the lattice induced potential $E_0/(1 + I_L)$ increases with E_0 increasing, and the SDGSs become more stable. A similar finding has been reported for vortex solitons in a saturable medium.[29]

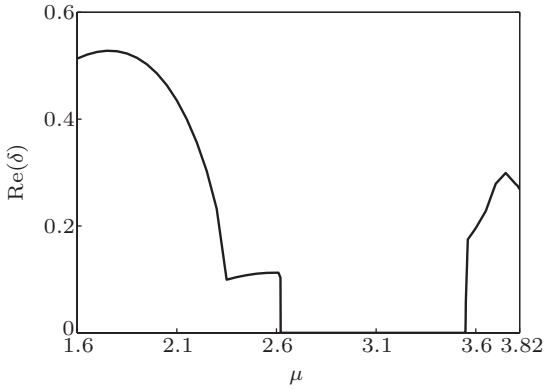


Fig. 4. Dependence of Re(δ) on μ for $\varepsilon = -0.5$ and $E_0 = 6.5$.

We increase the depth of the repulsive defect and choose $\varepsilon = -1$, and plot the P–μ diagram and Re(δ)–μ curve in Figs. 5(a) and 5(b), respectively. The P–μ relationship in the SI gap is not shown in the figure, since the SDGSs are always not stable in this gap. As shown in Fig. 5(a), the soliton power first decreases exponentially and then increases at $\mu = 4.946$, after having reached a peak value (not apparent in the figure), the power exhibits a similar decrease behaviour. According to the VK criterion, there might be two stable regions, but surprisingly, only one stable region ($4.479 < \mu < 4.944$) exists under moderate soliton power in the first gap, because Re(δ) < 0 in this region as shown in Fig. 5(b). One may note that the stable region is narrower than that in the bulk case.[16] As we have done previously, in order to verify the analytic prediction, the excitations of SGDSs for different propagation constants are illustrated in Figs. 5(c)–5(e) (stable for $\mu = 4.75$), Figs. 5(f)–5(h) (unstable for $\mu = 4.45$), and Figs. 5(i)–5(k) (unstable for $\mu = 5.35$), respectively.

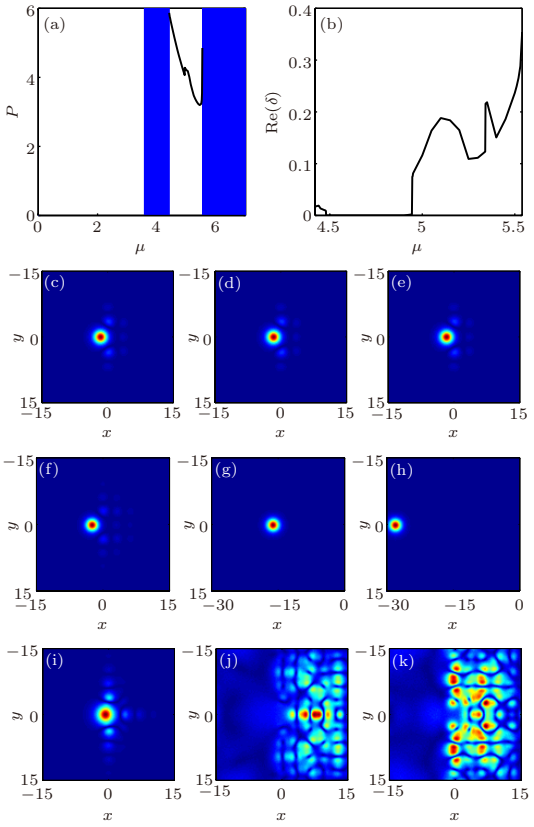


Fig. 5. (colour online) (a) Power diagram of SDGSs (dark regions correspond to Bloch bands). (b) Re(δ) versus μ. (c)–(k) Profiles of SDGS for (c) $\mu = 4.75$, $z = 0$; (d) $\mu = 4.75$, $z = 150$; (e) $\mu = 4.75$, $z = 300$; (f) $\mu = 4.45$, $z = 0$; (g) $\mu = 4.45$, $z = 150$; (h) $\mu = 4.45$, $z = 300$; (i) $\mu = 5.35$, $z = 0$; (j) $\mu = 5.35$, $z = 150$; (k) $\mu = 5.35$, $z = 300$. $\varepsilon = -1$.

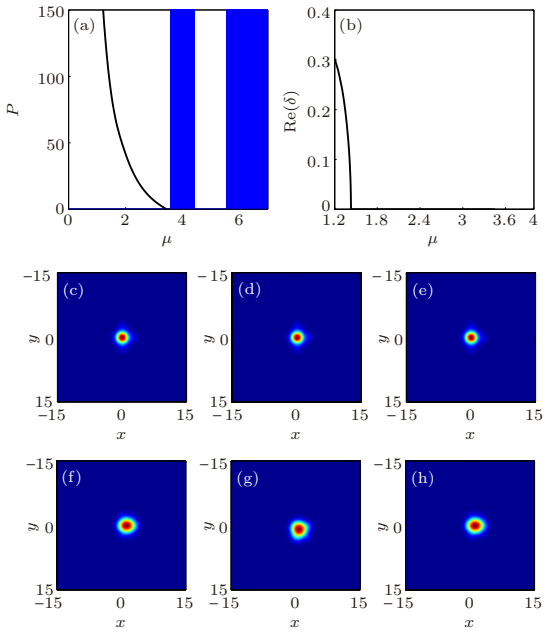


Fig. 6. (colour online) (a) Power diagram of SDGSs (dark regions correspond to Bloch bands). (b) Re(δ) versus μ. (c)–(h) Profiles of SDGS for (c) $\mu = 2.35$, $z = 0$; (d) $\mu = 2.35$, $z = 150$; (e) $\mu = 2.35$, $z = 300$; (f) $\mu = 1.25$, $z = 0$; (g) $\mu = 1.25$, $z = 150$; (h) $\mu = 1.25$, $z = 300$. $\varepsilon = 0.5$.

We turn to the attractive defect case and set $\varepsilon = 0.5$. By numerical evaluation, we find that there are no SGDSs existing in the first gap, so we shed light on the SGDSs existing in the SI gap. We plot the dependences of the soliton power P and the real part of the growth rate Re(δ) on propagation constant in Figs. 6(a) and 6(b), respectively. As shown in Fig. 6, the power decreases with propagation constant increasing, i.e., $\mathrm{d}P/\mathrm{d}\mu < 0$ in the SI gap, and there exists a stable region of $1.428 < \mu < 3.45$. The above prediction is justified by the direct simulation of Eq. (1), and the results are shown in Figs. 6(c)–6(e) (stable for $\mu = 2.35$) and Fig. 6(f)–(h) (unstable for $\mu = 1.25$). Comparing the case with the bulk case,[16] we notice that the stable region is even broader.

One of the interesting results is that the SDGSs do not require the threshold power for their excitation provided that the modulation depth of the defect intensity ε exceeds a critical value of 0.25 as shown in Fig. 7. When $\varepsilon \leq 0.25$, the P–μ dependence for SDGSs is non-monotonic and the slope of P–μ curve tends to infinity as the propagation constant approaches to the first band as shown in Fig. 7(a). Therefore, the existence of SDGSs requires a threshold power P_{th}. In contrast, for $\varepsilon > 0.25$, P_{th} vanishes as shown in Fig. 7(a). The above phenomena are analogous to the results proposed by Szameit *et al.*[22] in optical lattices of Kerr type. However, what differs from Ref. [22] is that for $\varepsilon > 0.25$ the stability domain of SDGSs decreases as ε increases (Fig. 8(a)).

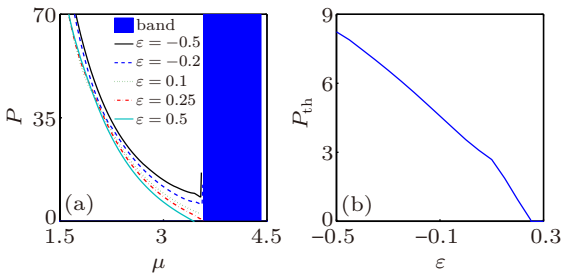


Fig. 7. (colour online) (a) Power diagrams of SDGSs versus μ for different values of ε in the SI band, and (b) threshold power P_{th} versus ε in the SI band.

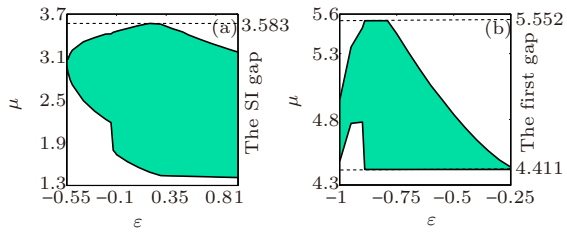


Fig. 8. Stability (shaded) and instability (white) regions of SDGSs for dependences of the propagation constant μ on defect parameter ε in (a) the SI gap and (b) the first gap.

Finally, after a huge of numerical work, we obtain the stability and instability regions of SDGSs for dependences of the propagation constant μ on defect parameter ε in the SI gap and the first gap as shown in Figs. 8(a) and 8(b), respectively. We find that the stable region of SDGSs existing in the SI gap for repulsive defect is narrower than that for the attractive defect. And when ε is less than a critical value (i.e., $\varepsilon = -0.55$), all the SDGSs are unstable in the SI gap. Similarly, there is a threshold value of ε (i.e., $\varepsilon = -0.24$), above which the powers of SDGSs in the first gap are nearly zero, i.e., the SDGSs are nonexistent. However it is worthwhile to remark that the SDGSs are stable in the whole first gap for the specific region of $0.79 < \varepsilon < 0.89$.

4. Conclusion

In this paper, we study SDGSs at an interface between a defect of 2D OLs and uniform saturable Kerr nonlinear medium. For repulsive defect, the SDGSs can exist in both SI gap and first gap. But in the SI gap, if ε is lower than a critical value, there will be no stable SDGSs. In the first gap, the power of SDGSs is almost zero provided that the defect parameter ε exceeds a threshold value. For the attractive defect, SDGSs exist only in SI gap and are stable in the low power region.

References

[1] Yeh P, Yariv A and Cho A Y 1978 *Appl. Phys. Lett.* **32** 104

[2] Shadrivov I V, Sukhorukov A A and Kivshar Y S 2003 *Phys. Rev.* E **67** 057602

[3] Makris K G, Suntsov S, Christodoulides D N, Stegeman G I and Hache A 2005 *Opt. Lett.* **30** 2466

[4] Suntsov S, Makris K G, Christodoulides D N, Stegeman G I, Hache A, Morandotti R, Yang H, Salamo G and Sorel M 2006 *Phys. Rev. Lett.* **96** 063901

[5] Makris K G, Hudock J, Christodoulides D N, Stegeman G I, Manela O and Segev M 2005 *Opt. Lett.* **30** 2466

[6] Kartashov Y V, Vysloukh V A and Torner L 2006 *Phys. Rev. Lett.* **96** 073901

[7] Rosberg C R, Neshev D N, Krolikowski W, Mitchell A, Vicencio R A, Molina M I and Kivshar Y S 2006 *Phys. Rev. Lett.* **97** 083901

[8] Szameit A, Kartashov Y V, Dreisow F, Persch T, Nolte S, Tünnermann A and Torner L 2007 *Phys. Rev. Lett.* **98** 173903

[9] Wang X, Bezryadina A, Chen Z, Makris K G, Christodoulides D N and Stegeman G I 2007 *Phys. Rev. Lett.* **98** 123903

[10] Szameit A, Kartashov Y V, Dreisow F, Heinrich M, Vysloukh V A, Persch T, Nolte S, Tünnermann A, Lederer F and Torner L 2008 *Opt. Lett.* **33** 663

[11] Alfassi B, Rotschild C, Manela O, Segev M and Christodoulides D N 2007 *Phys. Rev. Lett.* **98** 213901

[12] Huang H C, He Y J and Wang H Z 2009 *Chin. Phys.* B **18** 4919

[13] Fedele F, Yang J and Chen Z 2005 *Opt. Lett.* **30** 1506

[14] Yang J and Chen Z 2006 *Phys. Rev.* E **73** 026609

[15] Wang J, Yang J and Chen Z 2007 *Phys. Rev.* A **76** 013828

[16] Chen W, Zhu X, Wu T and Li R 2010 *Opt. Express* **18** 10956

[17] Zhu X, Wang H and Zheng L 2010 *Opt. Express* **18** 20786

[18] Dong L and Ye F 2010 *Phys. Rev.* A **82** 053829

[19] Yang X Y, Zheng J B and Dong L W 2011 *Chin. Phys.* B **20** 034208

[20] Wang X, Young J, Chen Z, Weinstein D and Yang J 2006 *Opt. Express* **14** 7362

[21] Makasyuk I, Chen Z and Yang J 2006 *Phys. Rev. Lett.* **96** 223903

[22] Szameit A, Kartashov Y V, Heinrich M, Dreisow F, Persch T, Nolte T S, Tünnermann A, Lederer F, Vysloukh V A and Torner L 2009 *Opt. Lett.* **34** 797

[23] Chen W, He Y, and Wang H 2006 *Opt. Express* **14** 11271

[24] Zhu W, Luo L, He Y and Wang H 2009 *Chin. Phys.* B **18** 4319

[25] Fleischer J W, Segev M, Efremidis N K and Christodoulides D N 2003 *Nature* **422** 147

[26] Yang J and Lakoba T I 2007 *Stud. Appl. Math.* **118** 153

[27] Yang J 2008 *J. Comput. Phys.* **227** 6862

[28] Vakhitov M G and Kolokolov A A 1973 *Sov. J. Radiophys. Quantum. Electron.* **16** 783

[29] Yang J 2004 *New. J. Phys.* **6** 47